

High Atmospheric Nitrate Inputs and Nitrogen Turnover in Semi-arid Urban Catchments

Krystin M. Riha,¹ Greg Michalski,^{1,2*} Erika L. Gallo,^{3,4} Kathleen A. Lohse,⁴ Paul D. Brooks,³ and Tom Meixner³

¹Department of Earth, Atmospheric, and Planetary Sciences, Purdue University, 550 Stadium Mall Drive, West Lafayette, Indiana 47907, USA; ²Department of Chemistry, Purdue University, 550 Stadium Mall Drive, West Lafayette, Indiana 47907, USA; ³Department of Hydrology and Water Resources, University of Arizona, Tucson, Arizona 85719, USA; ⁴Department of Biological Sciences, Idaho State University, Pocatello, Idaho 83209, USA

ABSTRACT

The influx of atmospheric nitrogen to soils and surfaces in arid environments is of growing concern due to increased N emissions and N usage associated with urbanization. Atmospheric nitrogen inputs to the critical zone can occur as wet (rain or snow) or dry (dust or aerosols) deposition, and can lead to eutrophication, soil acidification, and groundwater contamination through leaching of excess nitrate. The objective of this research was to use the $\delta^{15}\text{N}$, $\delta^{18}\text{O}$, and $\Delta^{17}\text{O}$ values of atmospheric nitrate (NO_3^-) (precipitation and aerosols) and NO_3^- in runoff to assess the importance of N deposition and turnover in semi-arid urban watersheds. Data show that the fractions of atmospheric NO_3^- exported from all the urban catchments, throughout the study period, were substantially higher than in nearly all other ecosystems studied with mean atmospheric contributions of 38% (min 0% and max 82%). These results suggest that catchment and stream channel

imperviousness enhance atmospheric NO_3^- export due to inefficient N cycling and retention. In contrast, catchment and stream channel perviousness allow for enhanced N processing and therefore reduced atmospheric NO_3^- export. Overall high fractions of atmospheric NO_3^- were primarily attributed to slow N turn over in arid/semi-arid ecosystems. A relatively high fraction of nitrification NO_3^- (~30%) was found in runoff from a nearly completely impervious watershed (91%). This was attributed to nitrification of atmospheric NH_4^+ in dry-deposited dust, suggesting that N nitrifiers have adapted to urban micro niches. Gross nitrification rates based on $\text{NO}_3^- \Delta^{17}\text{O}$ values ranged from a low $3.04 \pm 2 \text{ kg NO}_3\text{-N km}^{-2} \text{ day}^{-1}$ in highly impervious catchments to a high of $10.15 \pm 1 \text{ kg NO}_3\text{-N km}^{-2} \text{ day}^{-1}$ in the low density urban catchment. These low gross nitrification rates were attributed to low soil C:N ratios that control gross autotrophic nitrification by regulating gross NH_4^+ production rates.

Key words: urban ecosystems; N cycle; isotopes; gross nitrification; N deposition; runoff.

Received 2 October 2013; accepted 2 May 2014

Electronic supplementary material: The online version of this article (doi:10.1007/s10021-014-9797-x) contains supplementary material, which is available to authorized users.

Author contributions Riha: data collection, isotope analysis, data interpretation, lead author Michalski: isotope analysis, data interpretation, lead author, advisor to Riha Lohse: field data collection, geochemical analysis, data interpretation, lead author Gallo: data collection, GIS analysis, data interpretation, co-author Brooks: field support, data collection, data interpretation, editor Meixner: data interpretation, meta data, modeling, editor.

*Corresponding author; e-mail: gmichals@purdue.edu

INTRODUCTION

Arid and semi-arid regions cover one-third of the Earth's terrestrial surface and are experiencing disproportionate increases in population growth and land-use change (Ezcurra 2006). These

alterations are straining already scarce water resources (Norman and others 2009), have altered catchment scale hydrologic regimes and are changing nitrogen biogeochemistry (Fenn and others 2003a, b; Hall and others 2011). For example, in most urban areas, flood control management has resulted in dense stormwater drainage systems that enhance catchment connectivity and increase storm runoff quantity. In addition, urban regions alter the N cycle through increased N emissions from fossil fuel combustion, N fertilizer use, and increased N mobility due to land-use change (Vitousek and others 1997). Elevated nitrogen inputs have been shown to critically alter plant and microbial community composition and contribute to declines of sensitive organisms in both terrestrial and aquatic ecosystems (see Fenn and others 2003a for review). Studying urban catchments provides an integrated look at how key biogeochemical cycles, including the N cycle, function in a perturbed ecosystem (Lohse and others 2008). The effect of water and nitrogen reallocation on soil microbial processes and nutrients cycling in urbanized desert ecosystems, however, remains understudied (Lovett and others 2005). Fingerprinting nitrogen (N) sources and processes (that is, nitrification, nitrogen (N) deposition, and N leaching) and their feedbacks on ecosystem function and services can be used for developing science-based management strategies for sustaining these limited resources.

In many ecosystems, dissolved N in stream flow and storm runoff events predominately occurs as dissolved organic nitrogen (Worsfold and others 2008; Berman and Bronk 2003), followed by nitrate (NO_3^-) sourced from biological nitrification with only a small amount of NO_3^- sourced from the atmosphere (for example, Barnes and others 2008; Kendall and others 2007; Pardo and others 2004). In semi-arid urban regions, N loading to streams and waterways may increase due to increased N emissions (Fenn and others 2003b), increased imperviousness (Arnold and Gibbons 1996), and enhanced catchment connectivity due to storm water infrastructure (Carle and others 2005; Hatt and others 2004). Studies in semi-arid ecosystems have suggested an increase in microbial processing upon soil wetting, leading to an accumulation of soil nutrients (Austin and others 2004; Welter and others 2005). In addition to non-point sources such as fertilizer input and septic tank leaching, some studies show increases in soil NO_3^- likely due to nitrification between storm events in semi-arid urban catchments, which is quickly mobilized and flushed during runoff (Lewis and

Grimm 2007; McCrackin and others 2008; Gallo and others 2013a, b). Although elevated dry N deposition in urban areas has been documented in a number of studies (Fenn and others 2003a, b; Groffman and others 2004; Lohse and others 2008), the relative contributions and controls of biologically processed and atmospheric N loading to storm runoff have not been well quantified or identified. Differentiating between biologically processed (biologic, henceforth) and atmospherically sourced (atmospheric, henceforth) NO_3^- is not possible by simple mass balance, making it difficult to quantify their relative contributions to an ecosystem, and to assess how the importance of these NO_3^- sources change under water limitation or urbanization. There is a clear need for improved understanding and quantification of the N cycle in semi-arid urbanized ecosystems as related to N deposition, and more robust techniques to separate the relative contributions of different sources of N (Adams 2003).

Stable isotope abundance variations in NO_3^- can be useful in N biogeochemical studies as they can be used to infer changing NO_3^- sources or biogeochemistry. Research on atmospheric NO_3^- deposition in forested ecosystems using the dual-isotope approach ($\delta^{15}\text{N}$ and $\delta^{18}\text{O}$; for example, Durka and others 1994; Mayer and others 2002) suggest no atmospheric NO_3^- deposition despite high N deposition rates likely due to the high variability of the $\delta^{18}\text{O}$ values of biologic and atmospheric NO_3^- , which is often times a limiting factor in using the dual-isotope approach in mixed systems (Michalski and others 2004b). Atmospheric NO_3^- is known to be anomalously enriched in ^{17}O (Michalski and others 2003a). This ^{17}O enrichment is denoted by $\Delta^{17}\text{O}$, where $\Delta^{17}\text{O} = \delta^{17}\text{O} - 0.52(\delta^{18}\text{O})$ (Miller 2002). Atmospheric NO_3^- $\Delta^{17}\text{O}$ values have mainly been measured in coastal and ocean environments and range between 20 and 32‰ whereas NO_3^- produced by nitrification has a $\Delta^{17}\text{O} = 0$ ‰. NO_3^- loss processes (that is, denitrification and assimilation) obey the mass-dependent fractionation law which leaves the $\Delta^{17}\text{O}$ signal unaltered (Michalski and others 2004a). Therefore, $\Delta^{17}\text{O}$ can be used as a conservative tracer of atmospheric NO_3^- and can be used to better understand the fate of atmospheric deposition in semi-arid urbanized ecosystems, and can provide insights into the rate on microbial N turnover.

We hypothesized that semi-arid urban streams would have high amounts of atmospheric NO_3^- based on the following factors: first, urbanization increases local N emissions, in particular NO_x ($\text{NO} + \text{NO}_2$) generated by automobile exhaust

(Fenn and others 2003a, b) that is converted to NO_3^- in the atmosphere on relatively short time-scales (~ 1 day) and deposited locally (Munger and others 1998). Second, impervious surfaces reduce N residence time in urbanized catchments by facilitating rapid runoff. This would limit the ability of atmospherically deposited NO_3^- to infiltrate soil, therefore limiting NO_3^- loss by microbial cycling during transport. Third, increasing impervious surfaces in urban areas disrupt natural desert ecosystems, which may reduce nitrification potential in soils that already have low productivity relative to more temperate ecosystems. A decrease in biologically processed NO_3^- would result in atmospheric NO_3^- accounting for a larger fraction of NO_3^- in stream when soils are flushed during rain events.

Our objective is to use stable isotopes in NO_3^- to understand how microbial processing of nitrate in semi-arid regions compares to temperate regions and if urbanization enhances nitrate delivery to urban waterways. We address the following questions: (1) $\Delta^{17}\text{O}$ data for precipitation NO_3^- is not available for the southwestern US, therefore how do NO_3^- isotopic abundances in precipitation collected in a Tucson compare to other regions? (2) Is there significant atmospheric NO_3^- present in streamflow of semi-arid urban streams and how does that compare with temperate urban ecosystems? (3) Can additional information be obtained about N transformations through the coupled use of the $\delta^{18}\text{O}$ and $\Delta^{17}\text{O}$ methods of atmospheric NO_3^- tracers? (4) Can $\Delta^{17}\text{O}$ be used to obtain a gross nitrification rate in semi-arid urban catchments? To test this hypothesis and address the research questions, NO_3^- isotopes were analyzed in rainwater and runoff in six semi-arid urban catchments located in the southwestern United States.

Study Catchments

The study catchments were situated within the Tucson metropolitan area, AZ located in the southwestern United States. The current population of the Tucson metropolitan area is ~ 1 million residents (U.S. Census Bureau 2012). The Santa Catalina, Rincon, and Tucson Mountain range bound the Tucson metropolitan area forming an alluvial basin. The basin drains to the northeast by the ephemeral Santa Cruz River and its tributaries, the Canada del Oro, Rillito Creek, Pantano Wash, and Tanque Verde Creek (Davidson 1973). Climate in the Tucson basin is semi-arid with a mean annual temperature of 20°C (maximum 30°C in July and minimum 10°C in January). Mean annual

precipitation is approximately 310 mm and has a bimodal distribution. Approximately 50% of rainfall occurs during the winter and spring (November to March) in response to large storm systems that originate out of the Pacific Ocean. The second period of rainfall occurs during the summer months (the North American Monsoon), between June and September from storm systems originating from the Gulf of Mexico, the Pacific Ocean, and the Gulf of California (Gelt and others 1999). Summer rain events are short, intense, and spatially heterogeneous (Garcia and others 2008; Morin and others 2006; Syed and others 2003). Annual NO_x emissions (anthropogenic and biogenic) for Pima County totaled 32,000 ton (U.S. Environmental Protection Agency 2012) whereas modeled annual total N deposition was estimated at $7.5\text{--}15 \text{ kg N ha}^{-1} \text{ y}^{-1}$ (Fenn and others 2003b) and measured annual total N deposition for nearby Phoenix, AZ was $4\text{--}7 \text{ kg N ha}^{-1} \text{ y}^{-1}$ of which $1 \text{ kg N ha}^{-1} \text{ y}^{-1}$ was estimated to be NO_3^- (Lohse and others 2008).

Six catchments spanning a gradient of imperviousness (2.9–90.7%) and size (0.45–26.98 km^2) were used in this study (Table 1). Four of the urban catchments have been previously described and characterized by Gallo and others (2013a). Two additional catchments were added to this study and were delineated and characterized using the methods described by Gallo and others (2013a) in Arc-Map 9.3 using the storm water drainage system, which includes engineered, natural, impervious, and pervious waterways. There are no combined sewers or sewer overflow systems in the Tucson basin. All of these catchments are hydrologically isolated and do not receive water contributions from other sources. Characteristics for each study catchment are summarized in Table 1 and vary in land-use type, percent impervious cover, size, slope, and stream channel network.

METHODS

Rainfall and Runoff Sample Collection and Analyses

Rainfall data (rainfall depth, duration, time since last rainfall) were obtained from four Pima County Flood Alert system monitoring sites (2380, 2350, 6180, and 6190; <http://rfcd.pima.gov/wrd/alertsys/index.htm>) which were located in close proximity to the study catchments (Figure 1). Rainfall samples for isotope and inorganic N analyses were collected both for the 2007 and 2010 monsoons. Samples were collected by 21 citizen scientist

Table 1. Land Cover Characteristics of the Study Catchments

	Catchment					
	NU	LD	MD	MX1	MX2	CM
Catchment area (km ²)	26.98	4.44	0.45	4.7	25.30	0.33
Impervious cover (%)	2.92	21.84	40.64	45.78	50.63	90.70
Predominant land cover	Non-urban	Low density	Medium density	Mixed density	Mixed density	Commercial
Catchment slope (%)		5.60	1.20	1.90		1.50
Land cover (%)						
Residential housing						
Low density	3.29	87.56	0.13	11.08	3.92	0.32
Medium density	1.85	0.09	80.57	43.27	52.24	2.15
High density	0.75	7.26	16.70	17.28	11.22	0
Commercial (office, retail, roads)	1.66	5.00	2.59	19.76	27.36	95.65
Open space (parks, undeveloped)	92.45	0.08	0	2.78	5.26	1.87
Agriculture	0	0	0	5.54	0	0
Stream channel length (m)	146,474	12,479	881	18,634	70,496	1,457
Impervious channel length (m)	1,649	1,102	881	15,021	44,748	1457
Pervious channel length (m)	144,825	11,377	0	3,613	25,748	0

located throughout the Tucson Basin (Figure 1) in collaboration with Rainlog.org and the Sustainability of Semi-Arid Hydrology and Riparian Areas (SAHRA) Science and Technology Center at the University of Arizona (Gallo and others 2013b). Additional precipitation samples were also collected from rainfall collectors located at the outlet of the catchments during the 2010 summer monsoon. Rainfall samples were collected either through direct collection of rainfall into pre-cleaned HDPE

bottles and test tubes or by using a small funnel placed on the mouth of the collection container. Rainfall samples collected by citizen scientists were either picked up within 24 h or shipped for overnight delivery to the University of Arizona with ice packs supplied by our research team and were processed immediately upon arrival at the laboratory. Aliquots of 13 mL were immediately frozen for isotopic analyses. Aliquots for inorganic N analyses were stored with no headspace.

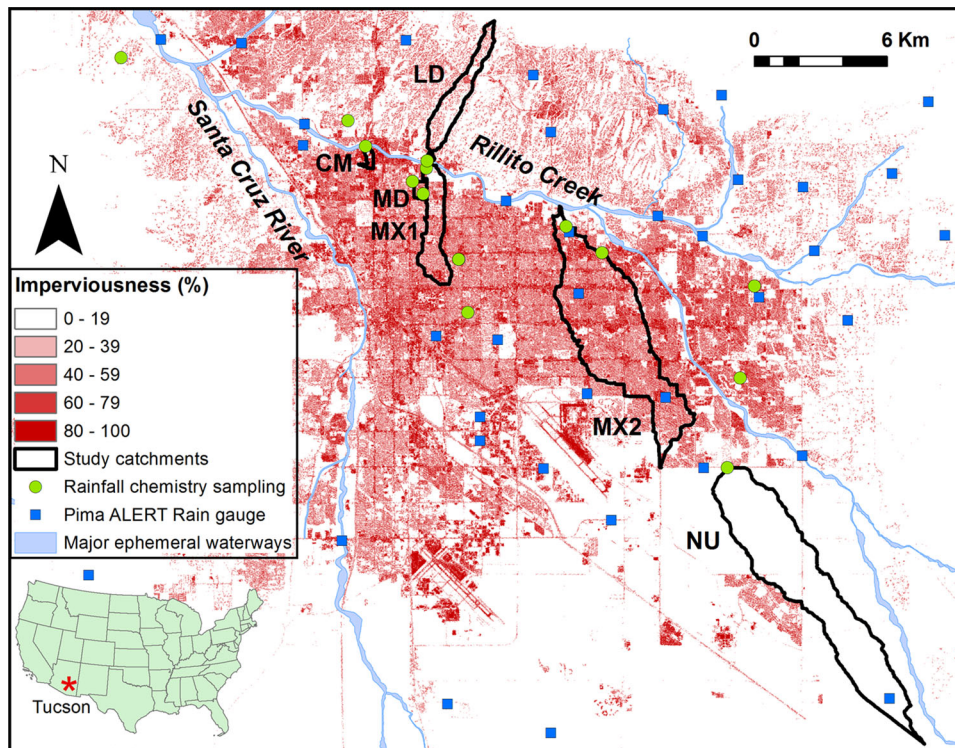


Figure 1. Location of the six study catchments: low density (LD), commercial (CM), medium density (MD), mixed land use 1 and 2 (MX₁ and MX₂), and non-urban (NU); tipping bucket rainfall gauges from the Pima County ALERT flood monitoring network (blue squares), rainfall sampling locations for nutrient and isotopic analyses (green circles) and percent impervious cover within the Tucson Basin in south-eastern Arizona (Color figure online).

Runoff samples were collected during the 2007, 2008, and 2010 summer monsoon seasons and analyzed for isotopes and geochemistry. Runoff was collected using automatic water samplers (ISCO 6712, Teledyne Technologies) installed at the outlet of each catchment. In 2007, they were programmed to collect a discrete sample every 20 min (for 4 h), and in 2010, once stage height exceeded 1 cm samples were collected every 10 min the first 40 min and every 20 min thereafter. Runoff samples were collected in acid washed combusted 1 L glassware (2007) or plastic bottles with ProPak disposable sample bags (2010). Samples (both runoff and rainfall positioned at the catchment outlet) were collected within 8 h after the runoff event, placed in a dark cooler ($\sim 4^\circ\text{C}$) and immediately taken to the University of Arizona for processing.

Rainfall and runoff samples were all processed similarly; a sample subset was filtered through a pre-combusted $0.7\text{-}\mu\text{m}$ glass fiber filter (Whatman GF/F) for nutrient and isotopic analyses. Aliquots for NO_3^- isotopic analysis were frozen shipped with ice packs overnight to Purdue Stable Isotope Facility (West Lafayette, IN). Ammonium-N analyses were carried out on a SmartChem Discrete Analyzer with a detection limit of 0.002 mg L^{-1} . Nitrite-N (NO_2^- -N) and NO_3^- -N analysis was carried out on a Dionex Ion Chromatograph ICS-5000 with a detection limit of 0.005 mg L^{-1} . All concentrations are reported as N (that is, NO_3^- -N and NH_4^- -N). Isotope analyses were performed using the denitrifier gold tube thermal reduction (Casciotti and others 2002; Kaiser and others 2007; Riha 2013) technique, where $\delta = (R_{\text{sample}}/R_{\text{standard}} - 1) \times 1000$ and R is the ratio of the rare isotope relative to the abundant isotope of the sample and the standard. Due to the non-selectivity of the denitrifier method, nitrite was removed from runoff and rainfall samples using the sulfamic acid method (Granger and Sigman 2009). Isotope ratios were measured using the Delta V Plus ratio mass spectrometer, which was calibrated using internal working reference standards that were previously calibrated to international standards USGS32, USGS35, and USGS34 (Riha 2013). All subsequent $\delta^{15}\text{N}$ values are reported versus air N_2 and oxygen values ($\delta^{18}\text{O}$ and $\Delta^{17}\text{O}$) are reported with respect to VSMOW. The anomalous ^{17}O enrichment, denoted by $\Delta^{17}\text{O}$, was determined using (Miller 2002):

$$\Delta^{17}\text{O} = \left[\ln\left(1 + \frac{\delta^{17}\text{O}}{1000}\right) - 0.52 \cdot \ln\left(1 + \frac{\delta^{18}\text{O}}{1000}\right) \right] \cdot 1000 \quad (1)$$

Precision of the $\delta^{15}\text{N}$ values were $\pm 0.4\text{‰}$, $\delta^{18}\text{O}$ values were $\pm 1.0\text{‰}$, and $\Delta^{17}\text{O}$ values were $\pm 0.3\text{‰}$

based on replicate analysis of the working standards and calibrations.

Isotopic Mass Balance

The fraction of atmospheric NO_3^- in urban runoff samples was determined using two mixing models, the first used $\Delta^{17}\text{O}$ values and the second used the $\delta^{18}\text{O}$ values. The first model employed the use of runoff NO_3^- . $\Delta^{17}\text{O}$ values to determine the fraction of atmospheric (f_{atm}) and biologic (f_{bio}) NO_3^- in a sample through the use of isotope mass balance:

$$\Delta^{17}\text{O}_{\text{runoff}} = f_{\text{bio}}(\Delta^{17}\text{O}_{\text{bio}}) + f_{\text{atm}}(\Delta^{17}\text{O}_{\text{atm}}), \quad (2)$$

where $\Delta^{17}\text{O}_{\text{runoff}}$, $\Delta^{17}\text{O}_{\text{bio}}$, and $\Delta^{17}\text{O}_{\text{atm}}$ are the isotopic compositions of NO_3^- in the urban runoff sample, biologically produced NO_3^- , and atmospherically produced NO_3^- (precipitation), respectively, and f_{atm} and f_{bio} are the NO_3^- mole fractions, which together equal 1. Atmospheric NO_3^- is known to be anomalously enriched in ^{17}O (Michalski and others 2003a) whereas NO_3^- produced by nitrification has a $\Delta^{17}\text{O} = 0$ and NO_3^- loss by denitrification/assimilation obey the mass-dependent fractionation law leaving the $\Delta^{17}\text{O}$ signal unaltered (Michalski and others 2004a). This allows the isotopic mass balance to be reduced to

$$f_{\text{atm}} = \Delta^{17}\text{O}_{\text{runoff}}/\Delta^{17}\text{O}_{\text{atm}} \quad (3)$$

and

$$f_{\text{bio}} = 1 - f_{\text{atm}}. \quad (4)$$

The second approach to determine the fraction of atmospheric NO_3^- in runoff used the $\delta^{18}\text{O}$ value as the atmospheric NO_3^- tracer (Chang and others 2002; Durka and others 1994; Kaushal and others 2011; Kendall 1998a; Mayer and others 2002) in a two-component isotope mixing model

$$f_{\text{atm}} = (\delta^{18}\text{O}_{\text{runoff}} - \delta^{18}\text{O}_{\text{nit}})/(\delta^{18}\text{O}_{\text{atm}} - \delta^{18}\text{O}_{\text{nit}}), \quad (5)$$

where $\delta^{18}\text{O}_{\text{runoff}}$, $\delta^{18}\text{O}_{\text{nit}}$, and $\delta^{18}\text{O}_{\text{atm}}$ are the isotopic compositions of NO_3^- in the urban runoff, produced from nitrification, and by atmospheric chemistry (precipitation), respectively, and again f_{atm} can be obtained from equation (4). A variety of models have been used to evaluate the $\delta^{18}\text{O}$ value of nitrification NO_3^- . The simplest assumes that O atoms from atmospheric O_2 ($\delta^{18}\text{O} = 23\text{‰}$ (Horibe and others 1973; Kroopnick and Craig 1972)) and soil water are incorporated into NO_3^- in a 1:2 ratio (Mayer and others 2001). This ratio value has been recently challenged (Snider and others 2010) suggesting that oxygen exchange between H_2O and

NO_2^- controls the water to air incorporation ratio. However, it is likely that oxygen exchange between H_2O and NO_2^- would be minimal in these catchments due to the neutral to slightly basic soil conditions (7.5 ± 0.5), which limits the pH-dependent exchange rate (Bunton and others 1959) and the relatively small timescale that soil water is available in these semi-arid systems. Applying the 2:1 factor and using local precipitation water $\delta^{18}\text{O}$ values of $-5.6 \pm 4\text{‰}$ (*unpublished data*) would result in a $\delta^{18}\text{O}_{\text{nit}}$ value of $4 \pm 2.6\text{‰}$.

These two mixing models were evaluated to determine f_{atm} (and f_{bio}) depending on the availability of isotope data for precipitation NO_3^- during a particular storm. We had three different rainfall data availability scenarios for any one runoff event: (1) rainfall isotope data available from a single sample for that runoff producing storm, (2) rainfall isotope data available from multiple locations throughout the Tucson basin for that runoff event, and (3) no rainfall isotope data for that runoff event. In our first approach, if the runoff event had a single corresponding precipitation $\text{NO}_3^- \Delta^{17}\text{O}$ and $\delta^{18}\text{O}$ value, then these data were used in the isotopic mass balance model. In our second approach, for runoff events with multiple precipitation $\text{NO}_3^- \Delta^{17}\text{O}$ and $\delta^{18}\text{O}$ values available, the averaged $\Delta^{17}\text{O}$ and $\delta^{18}\text{O}$ values were used. In the third case, no precipitation NO_3^- was collected due to spatially heterogeneous distribution of rainfall. For example, whereas all catchments contained at least one rainfall collector at the outlet of the catchment, it was quite possible for it to rain at the upper portion of the catchment but to be dry at the outlet precipitation collector. In these cases, the seasonally averaged precipitation $\text{NO}_3^- \Delta^{17}\text{O}$ and $\delta^{18}\text{O}$ values were used. Uncertainties arising because of the assumptions in these three approaches are detailed in the discussion.

Nitrate fractional contributions (f_{atm} and f_{bio}) can be used to remove the isotopic influence of atmospheric NO_3^- from runoff samples (Dejwakh and others 2012; Michalski and others 2004b), which allows a better interpretation of the biological NO_3^- plotted in dual-isotope space. Dual-isotope plots of NO_3^- ($\delta^{15}\text{N}$ vs. $\delta^{18}\text{O}$) have been used to evaluate sources of N used during nitrification (Chen and MacQuarrie 2005; Kendall 1998b) and assess the degree of NO_3^- loss by denitrification or assimilation (Granger and others 2004). However, because $\delta^{18}\text{O}$ values of atmospheric NO_3^- are elevated but $\delta^{15}\text{N}$ values are similar to terrestrial sources, even a small f_{atm} can lead to scatter in a dual-isotope plot. Removing the atmospheric $\delta^{18}\text{O}$ and $\delta^{15}\text{N}$ components from runoff NO_3^- allows a better assessment

of other NO_3^- sources or loss by assimilation or denitrification. Therefore, the runoff NO_3^- samples were transformed using the observed $\Delta^{17}\text{O}$, $\delta^{15}\text{N}$, and $\delta^{18}\text{O}$ values of atmospheric NO_3^- to obtain $\delta^{15}\text{N}$ and $\delta^{18}\text{O}$ values of biologic NO_3^- (Dejwakh and others 2012). This isotope transform was applied to find the biological $\delta^{15}\text{N}$ and $\delta^{18}\text{O}$ values of NO_3^- using the following isotopic mass balances:

$$\delta^{18}\text{O}_{\text{bio}} = (\delta^{18}\text{O}_{\text{runoff}} - f_{\text{atm}}(\delta^{18}\text{O}_{\text{atm}}))/f_{\text{bio}} \quad (6)$$

$$\delta^{15}\text{N}_{\text{bio}} = (\delta^{15}\text{N}_{\text{runoff}} - f_{\text{atm}}(\delta^{15}\text{N}_{\text{atm}}))/f_{\text{bio}}. \quad (7)$$

To further assess differences amongst catchments the fraction of $[\text{NO}_3^-]$ derived from the atmosphere ($[\text{NO}_3^-]_{\text{atm}}$) compared to the biosphere ($[\text{NO}_3^-]_{\text{bio}}$) was calculated by

$$[\text{NO}_3^-]_{\text{atm}} = f_{\text{atm}}[\text{NO}_3^-] \quad (8)$$

and

$$[\text{NO}_3^-]_{\text{bio}} = f_{\text{bio}}[\text{NO}_3^-]. \quad (9)$$

Here we show that $\Delta^{17}\text{O}$ values can be used to estimate the gross nitrification rate (GNR) at the catchment scale. In essence, using $\Delta^{17}\text{O}$ to assess gross nitrification is analogous to ^{15}N isotope dilution techniques, but where the $\Delta^{17}\text{O}$ tracer is naturally applied. Because the main mechanisms controlling $[\text{NO}_3^-]$, denitrification, assimilation, and nitrification, are all mass-dependent isotope processes, the $\text{NO}_3^- \Delta^{17}\text{O}$ values remain unchanged under their influence. On the contrary, residual $\text{NO}_3^- \delta^{18}\text{O}$ values increase after NO_3^- loss by these processes and can be used to assess the importance of NO_3^- removal (net denitrification). To determine gross nitrification, an isotopic mass balance was calculated similar to that previously used to determine the NO_3^- fractional contributions

$$\Delta^{17}\text{O}_{\text{runoff}} = Q_{\text{bio}}(\Delta^{17}\text{O}_{\text{bio}}) + Q_{\text{atm}}(\Delta^{17}\text{O}_{\text{atm}}), \quad (10)$$

where Q_{bio} and Q_{atm} are now the gross rate fractions

$$Q_{\text{bio}} = \text{Gross nitrification rate} / (\text{gross nitrification rate} + \text{deposition rate}) \quad (11)$$

$$Q_{\text{atm}} = \text{Deposition rate} / (\text{gross nitrification rate} + \text{deposition rate}) \quad (12)$$

and

$$Q_{\text{atm}} = \Delta^{17}\text{O}_{\text{runoff}} / \Delta^{17}\text{O}_{\text{atm}} \quad (13)$$

and therefore

$$Q_{\text{bio}} + Q_{\text{atm}} = 1. \quad (14)$$

This model assumes that rainfall depth is heterogeneous across the study catchment and that all biologically produced NO_3^- in runoff is from dissolution and transport of near surface soil salts and therefore representative of nitrification occurring in the active layer since the last runoff event. It also assumes that there is sufficient exchange with the soil surface such that runoff would be representative of soil water (nitrification derived NO_3^-) and precipitation (atmospheric-derived NO_3^-). However, if overland flow is occurring, then poor exchange would be occurring and therefore GNR would be underestimated. The Q_{atm} (deposition rate) is the dry and wet deposition, with the dry rate being integrated over days since the previous rainfall. A constant dry deposition rate of $1.2 \text{ kg NO}_3\text{-N km}^{-2} \text{ day}^{-1}$ was used (Fenn and others 2003b). The amount of NO_3^- from daily wet deposition was obtained from the precipitation $[\text{NO}_3^-]$ and normalized to time between precipitation events. Substituting Q_{bio} and Q_{atm} into the original mass balance and solving for the gross nitrification rate yields (in units of $\text{kg NO}_3\text{-N km}^{-2} \text{ day}^{-1}$):

$$\text{Gross nitrification rate (GNR)} = Q_{\text{atm}} \cdot [1/(\Delta^{17}\text{O}_{\text{runoff}}/\Delta^{17}\text{O}_{\text{atm}}) - 1]. \quad (15)$$

Statistical Analyses

Statistical analyses were performed in JMP 10.0.0 (SAS System 2012). We used linear regression to identify if and how rainfall $\text{NO}_3\text{-N}$, ^{18}O and $\Delta^{17}\text{O}$ co-varied. Nonparametric pairwise Wilcoxon mean comparisons were used to determine if values of $\delta^{15}\text{N}$, $\delta^{18}\text{O}$, $\Delta^{17}\text{O}$, $\text{NO}_3\text{-N}$, $\text{NH}_4\text{-N}$, NO_3^- fractional contributions (f_{atm} and f_{bio}), the corresponding NO_3^- concentrations ($[\text{NO}_3^-]_{\text{atmo}}$ and $[\text{NO}_3^-]_{\text{bio}}$), as well as $\delta^{15}\text{N}_{\text{bio}}$, $\delta^{18}\text{O}_{\text{bio}}$ and gross nitrification rates varied significantly between catchments. In addition, we tested for differences in variances of $\delta^{15}\text{N}$ and f_{atm} across sites using the Levene's analyses of means (ANOM) for Variances. Finally, we used the unequal variance paired t test at each catchment to identify differences in f_{atm} estimated from the precipitation $\text{NO}_3^- \Delta^{17}\text{O}$ average or storm-specific $\text{NO}_3^- \Delta^{17}\text{O}$. All statistical comparisons were deemed significantly or "statistically" distinct at a significance level of $p < 0.05$.

RESULTS

Precipitation Isotopic and Geochemical Data

The $\Delta^{17}\text{O}$, $\delta^{18}\text{O}$, and $\delta^{15}\text{N}$ values of NO_3^- in precipitation varied spatially within storms and between consecutive storm events in Tucson during the study period (Figure 2). Between July 2009 and September 2010 ($n = 12$), rainfall $\text{NO}_3^- \Delta^{17}\text{O}$ values ranged from 20.3 to 30.6‰ and averaged 24.5‰. The $\delta^{18}\text{O}$ values ranged from 55.2 to 89‰, averaging 57‰, and the $\delta^{15}\text{N}$ values ranged from -4.2 to 2.6‰. There was a significant correlation ($p < 0.05$) between precipitation NO_3^- , $\delta^{18}\text{O}$, and $\Delta^{17}\text{O}$ values ($r^2 = 0.72$, slope = 0.25). Within the same storm event (July 19, 2010), a large spatial variation in $\text{NO}_3^- \Delta^{17}\text{O}$ (22.1–30.6‰), $\delta^{18}\text{O}$ (63.1–89‰), and $\delta^{15}\text{N}$ (-4.2 to 1.3‰) values was observed. The inter-storm $\text{NO}_3^- \delta^{18}\text{O}$ and $\Delta^{17}\text{O}$ correlation was significant and similar to the seasonal ($r^2 = 0.69$, slope = 0.21). Isotope data for precipitation NO_3^- were not obtained for all storms during the summer because of either limited rainfall or low NO_3^- concentration resulted in insufficient

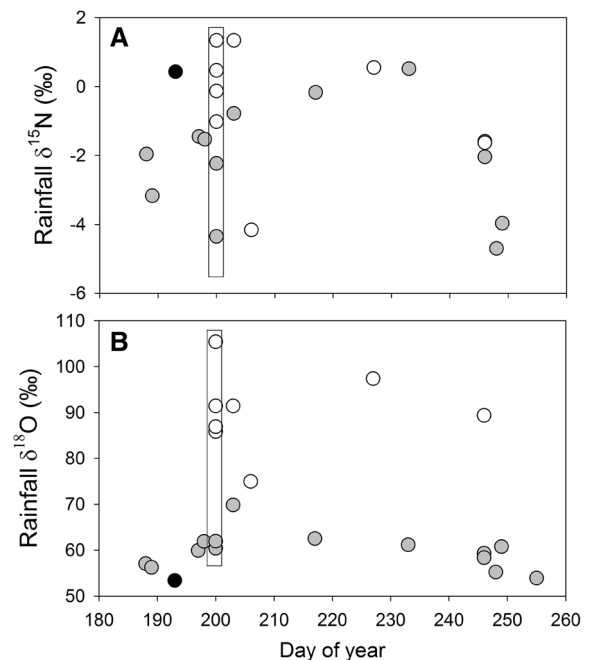


Figure 2. Values of **A** $\delta^{15}\text{N}$ and **B** $\delta^{18}\text{O}$ of NO_3^- in precipitation collected throughout the Tucson Basin during the study period (June to September, day of year 180–260). *Black circles* denote samples collected in 2008, *white circles* denote samples collected in 2009, and *gray circles* denote samples collected in 2010. *Box* encloses samples collected on day of year 200 which highlight the inter-annual and within-storm variability of the isotopic composition of rainfall within the Tucson basin.

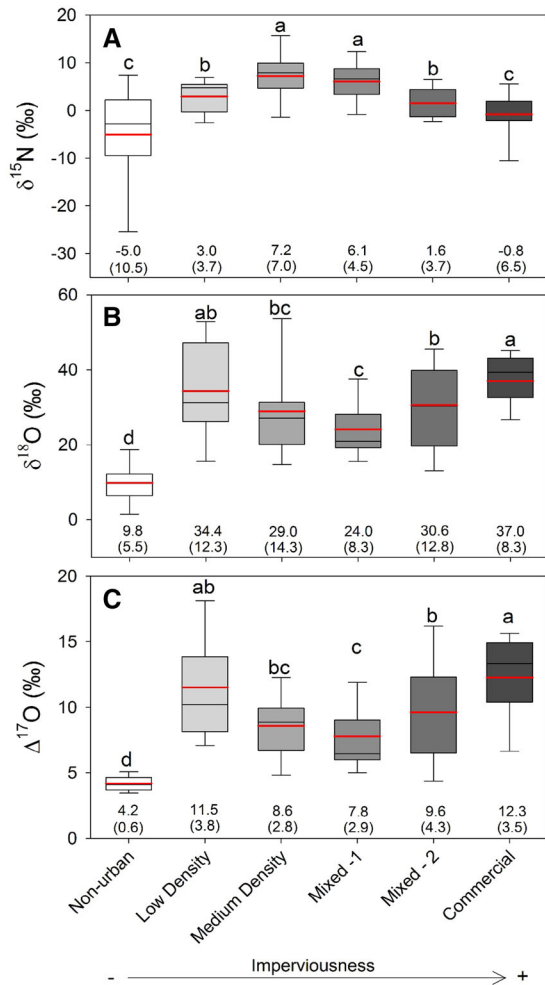


Figure 3. Box plots for each catchment showing runoff NO_3^- values of **A** $\delta^{15}\text{N}$, **B** $\delta^{18}\text{O}$, and **C** $\Delta^{17}\text{O}$. Catchment mean (SD) is shown below each box plot. Box plot red lines denote mean, thin black lines median. Box plots with distinct letters are significantly ($p < 0.05$) different.

NO_3^- for isotopic analysis. Precipitation $[\text{NO}_3^-\text{-N}]$ ranged from 0.005 to 2 mg L^{-1} (mean 0.4 mg L^{-1}) and $[\text{NH}_4^+\text{-N}]$ ranged from 0.002 to 5.5 mg L^{-1} (mean 0.8 mg L^{-1}). Rainfall $\text{NH}_4^+/\text{NO}_3^-$ ratios ranged from 0 to 2 (mean = 0.9).

Runoff Isotopic and Geochemical Data

Both $\delta^{18}\text{O}$ and $\Delta^{17}\text{O}$ values in runoff NO_3^- were high across all catchments (Figure 4; Table S2). The highest $\delta^{18}\text{O}$ and $\Delta^{17}\text{O}$ values were observed in the most and least impervious catchments, CM ($37.0\text{‰} \pm 8.3$ and $12.3\text{‰} \pm 3.5$, respectively) and LD ($34.4\text{‰} \pm 12.3$ and $11.5\text{‰} \pm 3.8$, respectively); whereas the NU catchment had the significantly lower $\delta^{18}\text{O}$ and $\Delta^{17}\text{O}$ values than all other sites ($9.8\text{‰} \pm 5.5$ and $4.2\text{‰} \pm 0.6$, respectively). The range in runoff NO_3^- $\delta^{15}\text{N}$ values within the

catchments was highly variable and many were outside the previously published $\delta^{15}\text{N}$ ranges for soil and stream NO_3^- (Kendall and others 2007). Statistically ($p < 0.05$), the highest $\delta^{15}\text{N}$ values were observed in MX_1 ($6.1\text{‰} \pm 4.5$) and MD ($7.2\text{‰} \pm 7.0$) whereas the lowest were observed in NU ($-5.0\text{‰} \pm 10.5$) and CM ($-0.8\text{‰} \pm 6.5$). In addition, we found that $\delta^{15}\text{N}$ values were statistically more variable at NU than at any other site ($\sigma = 110.4$). Concentrations of NO_3^- -N were statistically highest at CM ($1.1 \text{ mg L}^{-1} \pm 0.4$) and LD ($1.1 \text{ mg L}^{-1} \pm 0.2$), and lowest at NU ($0.3 \text{ mg L}^{-1} \pm 0.1$; $p < 0.05$; Table S2). Similarly, NH_4^+ -N concentrations were statistically highest at CM ($0.6 \text{ mg L}^{-1} \pm 0.3$) and MD ($0.6 \text{ mg L}^{-1} \pm 0.4$) and lowest at NU ($0.02 \text{ mg L}^{-1} \pm 0.02$) (Figure 3).

Atmospheric NO_3^- Fractional Contribution Based on $\Delta^{17}\text{O}$

The f_{atm} was overall variable across all study catchments (mean = 0.38 ± 0.16 , $n = 179$) and differed slightly depending on which model (precipitation NO_3^- $\Delta^{17}\text{O}$ average or storm-specific) was used to calculate f_{atm} . Statistically ($p < 0.05$), the highest f_{atm} was observed at CM (0.49 ± 0.1) and the lowest and significantly less variable f_{atm} was observed at NU (0.17 ± 0.02) relative to the other catchments (Figure 4). The differences among catchments in the corresponding fraction weighted NO_3^- concentrations were statistically more distinct across sites (Figure 4). Specifically, significantly higher $[\text{NO}_3^-]_{\text{atm}}$ was found in the CM ($0.56 \pm 0.2 \text{ mg L}^{-1}$) and LD ($0.51 \pm 0.2 \text{ mg L}^{-1}$) catchments than in the any other catchment; whereas NU had a significantly lower $[\text{NO}_3^-]_{\text{atm}}$ than any other site ($0.06 \pm 0.02 \text{ mg L}^{-1}$). In contrast, there was more statistical overlap in $[\text{NO}_3^-]_{\text{bio}}$ across sites (LD, MD, MX_1 , MX_2 , and CM) with the exception of NU, which had significantly lower $[\text{NO}_3^-]_{\text{bio}}$ than any other site ($0.28 \pm 0.1 \text{ mg L}^{-1}$).

Biologically Produced NO_3^- Sources and Processing

Most of the transformed $\delta^{15}\text{N}_{\text{bio}}$ and $\delta^{18}\text{O}_{\text{bio}}$ values fell within the range of NO_3^- derived from nitrification in soils (Kendall and others 2007; Figure 5; Table S2). Values of $\delta^{15}\text{N}_{\text{bio}}$ at catchments MD ($13.7\text{‰} \pm 16.7$) and MX_1 ($9.3\text{‰} \pm 6.5$) were significantly more enriched in ^{15}N than the other study catchments; whereas NU ($-5.6\text{‰} \pm 12.5$) was significantly more depleted in ^{15}N than all but CM ($-0.5\text{‰} \pm 11.5$). Values of $\delta^{18}\text{O}_{\text{bio}}$ were significantly higher at the CM ($13.57\text{‰} \pm 11.8$) and

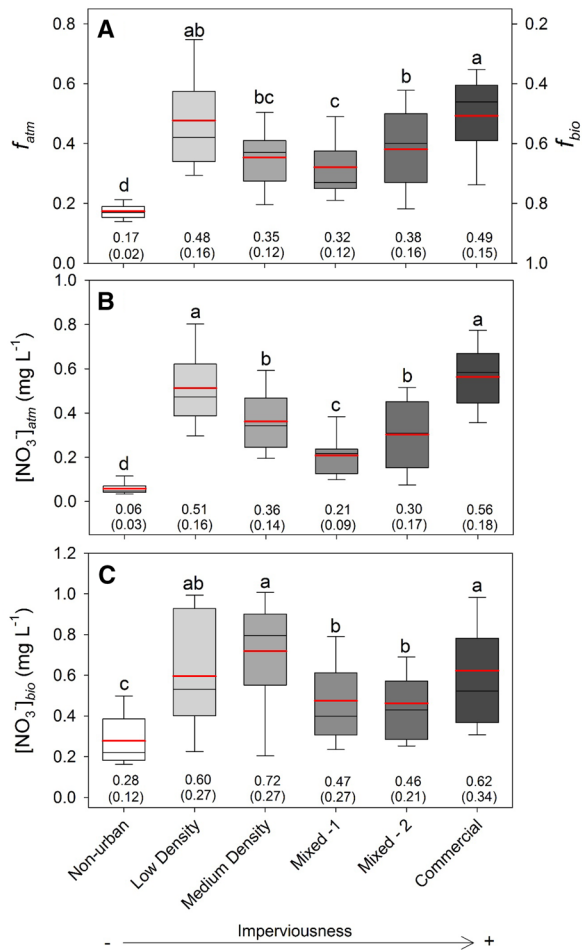


Figure 4. Box plots for each catchment showing **A** the runoff fraction of atmospheric NO_3^- (f_{atm} , left y-axis; f_{bio} , fraction biologic NO_3^- on right y-axis), concentration of **B** atmospherically and **C** biologically derived nitrate ($[NO_3^-]_{atm}$ and $[NO_3^-]_{bio}$, respectively) where $[NO_3^-]_{atm} = f_{atm} * [NO_3^-]$. Catchment mean (SD) is shown below each box plot, means in **A** are for f_{atm} . Box plot red lines denote mean, thin black lines median. Box plots with distinct letters are significantly ($p < 0.5$) different.

LD ($16.3\% \pm 14.8$) catchments than at MX₁, MX₂, and NU ($8.8\% \pm 7.0$, $4.4\% \pm 13.4$, and $-0.1\% \pm 6.2$, respectively) but not distinct from MD values ($16.8\% \pm 23.7$). Denitrification and assimilation were assessed through the use of the dual-isotope plot and NO_3^- processing was not detected in any of the study catchments.

DISCUSSION

Precipitation NO_3^- $\Delta^{17}O$ and $\delta^{18}O$ values

The precipitation NO_3^- $\delta^{18}O$ and $\Delta^{17}O$ values had a surprisingly high degree of variability in time and

space (Figure 2). Although the range of $\Delta^{17}O$ and $\delta^{18}O$ values were similar to those reported in Southern California (Michalski and others 2003b; Michalski and others 2004b), and $\delta^{18}O$ values were also comparable to those observed in the North-eastern United States (Burns and others 2009; Elliott and others 2009), the 7‰ $\Delta^{17}O$ and 30‰ $\delta^{18}O$ shift for NO_3^- in the same storm has yet to be reported. This is because most studies do not generally collect rain samples at a high spatial and temporal resolution as was done in this study.

There are two potential explanations for the spatiotemporal variability of NO_3^- isotopes in rainfall: (1) localized changes in NO_x chemistry based on the position of the precipitation collector and (2) Differences in the amount of wash out of particulate nitrate or gaseous HNO_3 in the rainfall samples. The range of precipitation NO_3^- $\Delta^{17}O$ values reported here suggests site-specific differences in HNO_3 formation pathways (Michalski and others 2003b). This variation may be due to heterogeneity of NO_x and VOC emissions within the Tucson Basin (Diem and Comrie 2001), such that during a precipitation event the time scale for local NO_x emissions to be converted into HNO_3 and subsequent deposition is short relative to mixing across the Tucson basin. Unfortunately, there was not enough data ($n = 12$) to determine trends in precipitation NO_3^- $\Delta^{17}O$ and $\delta^{18}O$ values throughout the course of the summer monsoon season. An alternate explanation is that the wash-out efficiency of particulate nitrate or gaseous HNO_3 is different in space a time. It has been shown that different sized NO_3^- particles and gaseous HNO_3 have different $\delta^{18}O$ and $\Delta^{17}O$ values (Freyer 1991; Morin and others 2009). Rainwater NO_3^- is a mixture of cloud water NO_3^- plus particulate NO_3^- and HNO_3 incorporated into the rain as it passes through the boundary layer, the later two diminishing in importance once the boundary layer has been cleansed by the precipitation. Differences in the proportion of cloud NO_3^- to washout NO_3^- could then explain the observed $\delta^{18}O$ and $\Delta^{17}O$ variations. It is unlikely the intra-storm differences are from isotope fractionation of dry-deposited particulate $NO_3^-_{(s)}$ and $HNO_3_{(g)}$ on the collection funnel because of its small surface area and any fractionation would likely obey the mass-dependent fractionation law, leaving the $\Delta^{17}O$ unaltered (Michalski and others 2004b). Therefore, we hypothesize that the $\delta^{18}O$ and $\Delta^{17}O$ variation most likely is a reflection of changes in NO_x chemistry based on the location of the precipitation collector (near road vs. residential area) within the Tucson Basin. These variations also

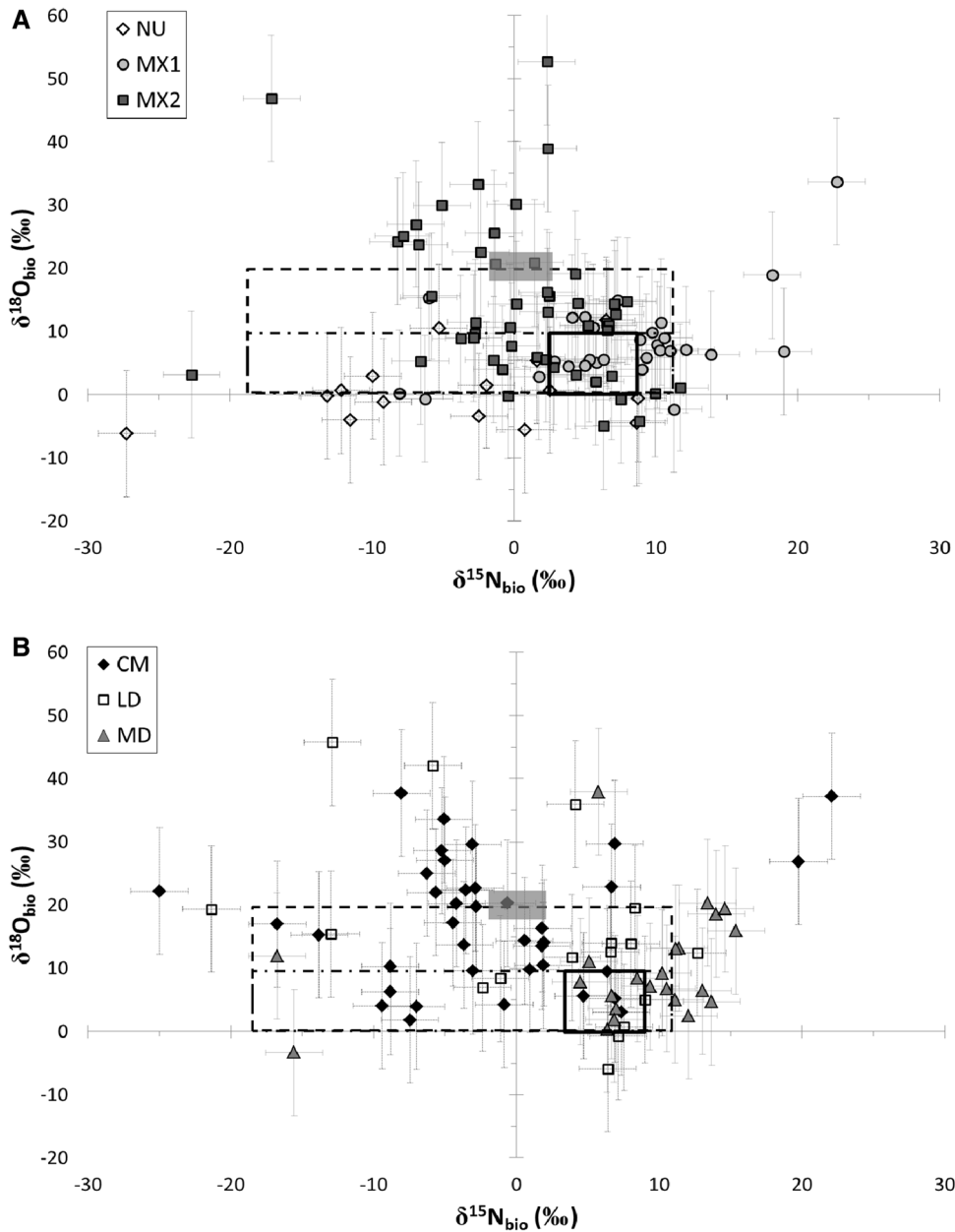


Figure 5. Dual-isotope plot of $\delta^{15}\text{N}$ and $\delta^{18}\text{O}$ values of non-atmospheric NO_3^- obtained by the $\Delta^{17}\text{O}$ transform of NO_3^- collected from catchments NU, MX1, and MX2 **A** and CM, LD, and MD **B**. Error bars represent the possible range of transformed $\delta^{15}\text{N}$ and $\delta^{18}\text{O}$ values based on the in the rainfall NO_3^- $\delta^{15}\text{N}$ and $\delta^{18}\text{O}$ ranges observed. Boxes encompass a range of values for a given N sources: the *dashed-dot box* is soil NH_4^+ , *solid box* is soil NO_3^- , *dashed box* includes $\delta^{18}\text{O}$ enrichment of soil water that could be used in nitrification and known fractionation factor (α) that occur during evaporation (Walker and others 1988) and the *shaded box* shows the range of synthetic fertilizer.

result in uncertainties when averaged precipitation NO_3^- $\Delta^{17}\text{O}$ and $\delta^{18}\text{O}$ values are used to estimate f_{bio} and f_{atm} in the absence of actual event-based data. Errors induced by utilization of seasonal averaged precipitation NO_3^- $\Delta^{17}\text{O}$ and $\delta^{18}\text{O}$ values versus event-based can be both large and variable ($\Delta^{17}\text{O}$: +3 to -10‰ and $\delta^{18}\text{O}$: -9 to -45‰).

Atmospheric NO_3^- in Runoff

The fraction of atmospheric NO_3^- exported from all of the urban catchments throughout the study period was substantially higher (regardless of $\Delta^{17}\text{O}$ or $\delta^{18}\text{O}$ approach) than nearly all other ecosystems

previously studied. Most studies quantifying atmospheric NO_3^- export have used elevated $\delta^{18}\text{O}$ values (50–90‰) in atmospheric NO_3^- as the tracer, have focused on forested and alpine ecosystems, and have shown little to no contribution of atmospheric NO_3^- to total N. Across 16 major watersheds in the northeastern U.S., atmospheric NO_3^- contributions were considered negligible because high microbial N cycling erased the atmospheric $\delta^{18}\text{O}$ tracer (Mayer and others 2002). In temperate forested ecosystems, atmospheric NO_3^- contributed 1–30% of total stream NO_3^- (Barnes and others 2008; Campbell and others 2006; Spoelstra and others 2001; Williard and others

2001). Unlike these forested catchments, all but one of our urban catchments, NU which is 92% undeveloped desert, had a significant fraction of atmospheric NO_3^- (averaging 34–53%).

The high $f_{\text{atm}} \text{NO}_3^-$ in runoff observed in Tucson (Figure 4) has been found in several ecosystems with perennial waterways, but often as transient pulses during peak discharge with low $f_{\text{atm}} \text{NO}_3^-$ observed during baseflow conditions. During peak snowmelt in forested watersheds, 45–48% of the NO_3^- load was atmospheric NO_3^- but not more than 7% during the majority of flow conditions (Goodale and others 2009; Pardo and others 2004; Sebestyen and others 2008). Similarly, $\Delta^{17}\text{O}$ was used in the Colorado Front range (Darroutzet-Nardi and others 2012) and semi-arid Southern California (Michalski and others 2004b) to show that initial runoff NO_3^- had a high atmospheric fraction but this quickly decreased to approximately 12%. These high atmospheric NO_3^- fractions during peak flow were primarily attributed to flushing of atmospheric NO_3^- deposition (for example, plants and soil) during prolonged dry periods. By contrast, in Tucson the fraction of atmospheric NO_3^- was very high during initial discharge and remained elevated throughout the hydrographs.

The difference in the amount of atmospheric NO_3^- in Tucson runoff relative to other mainly forested ecosystems in urban regions was likely a function of N deposition and cycling rates. NO_3^- deposition in northeastern US watersheds was estimated at 4–8 kg N $\text{ha}^{-1} \text{y}^{-1}$ (Mayer and others 2002), which is higher than both the modeled NO_3^- deposition rate (4 kg N $\text{ha}^{-1} \text{y}^{-1}$) in Tucson (Fenn and others 2003b) and the measured rate (1 kg N $\text{ha}^{-1} \text{y}^{-1}$) in Phoenix (Lohse and others 2008), a nearby urban desert. Therefore, major differences in atmospheric NO_3^- deposition rates between Tucson and eastern forests cannot explain higher atmospheric NO_3^- in Tucson's runoff. This suggests that the high amounts of atmospheric NO_3^- were due to decreased rates of assimilation/denitrification of deposited N and reduced nitrification rate in the semi-arid urban catchments. This supports our hypothesis that imperviousness limits N residence times and reduces the amount of exposed soil, thus and reduces N turnover rates.

Assessing f_{atm} Using $\delta^{18}\text{O}$ Versus $\Delta^{17}\text{O}$

Comparing the $\Delta^{17}\text{O}$ and $\delta^{18}\text{O}$ mass balance approaches to determine f_{atm} (Figure 6) yields additional information about the varying importance of nitrification within urban catchments. There was a strong correlation ($r^2 = 0.71$) between methods

suggesting that the primary mechanism controlling runoff $\text{NO}_3^- \delta^{18}\text{O}$ and $\Delta^{17}\text{O}$ values in Tucson runoff was likely the same, that is, deposition of atmospheric NO_3^- . However, the $\delta^{18}\text{O}$ method usually resulted in higher estimates of f_{atm} by approximately 10% and overestimations/underestimations of f_{atm} were ubiquitous and could be quite large ($\pm 40\%$) suggesting secondary mechanisms are altering the runoff $\text{NO}_3^- \delta^{18}\text{O}$ values (Figure 6). In catchments where f_{atm} was high (CM, LD, MD), the $\delta^{18}\text{O}$ method often over predicts f_{atm} relative to $\Delta^{17}\text{O}$. In catchments where f_{atm} was low (MX₁ and MX₂), the $\delta^{18}\text{O}$ method was comparable to the $\Delta^{17}\text{O}$ method, and in the non-urbanized NU catchment, the $\delta^{18}\text{O}$ method under predicted f_{atm} .

There should be a 1:1 correlation if the $\delta^{18}\text{O}$ and $\Delta^{17}\text{O}$ methods provide the same f_{atm} , and deviations from the 1:1 may indicate biologic NO_3^- or secondary mass-dependent isotope fractionations. We hypothesize that deviations from the 1:1 are most likely due to seasonal variability in the $\delta^{18}\text{O}_{\text{nit}}$ values themselves.

Fluctuations in $\delta^{18}\text{O}_{\text{nit}}$ values can be attributed to seasonal changes in Tucson precipitation $\delta^{18}\text{O}$ values, particularly during the transition to the monsoon seasons (Wright 2001). The variation of Tucson $\text{H}_2\text{O} \delta^{18}\text{O}$ values is a function of moisture sources (Pacific vs. Gulfs of Mexico/California), storm size (large—sourced outside basin, small—recycled within basin) and rain magnitude (Wright 2001). If nitrification occurs after a previous storm with a lower precipitation $\delta^{18}\text{O}$ value relative to the precipitation generating the runoff, then f_{atm} would be overestimated due to improper calculation of the $\delta^{18}\text{O}_{\text{nit}}$ value. Conversely, evaporation leads to elevated soil water $\delta^{18}\text{O}$ values (Gazis and Feng 2004), so if nitrification occurs after evaporative loss of soil water, f_{atm} calculated using $\delta^{18}\text{O}$ values would be underestimated because the $\text{H}_2\text{O} \delta^{18}\text{O}$ value would be too low. The observed deviations are not likely caused by variability of $\delta^{18}\text{O}_{\text{atm}}$ because the atmospheric $\text{NO}_3^- \delta^{18}\text{O}/\Delta^{17}\text{O}$ value ratio remains relatively constant during the summer monsoon season (Figure 2). Any inter-storm deviation in the $\delta^{18}\text{O}_{\text{atm}}$ value would also change the $\Delta^{17}\text{O}_{\text{atm}}$ value and thus alter the f_{atm} value by the same amount. Thus, the deviation from the 1:1 line in the f_{atm} plot suggests that there is varying importance of nitrification within each catchment that is being reflected in the $\text{NO}_3^- \delta^{18}\text{O}$ values.

One test of the hypothesis is that the variance in the 1:1 plot should increase in watersheds where higher fractions of soil nitrification might be

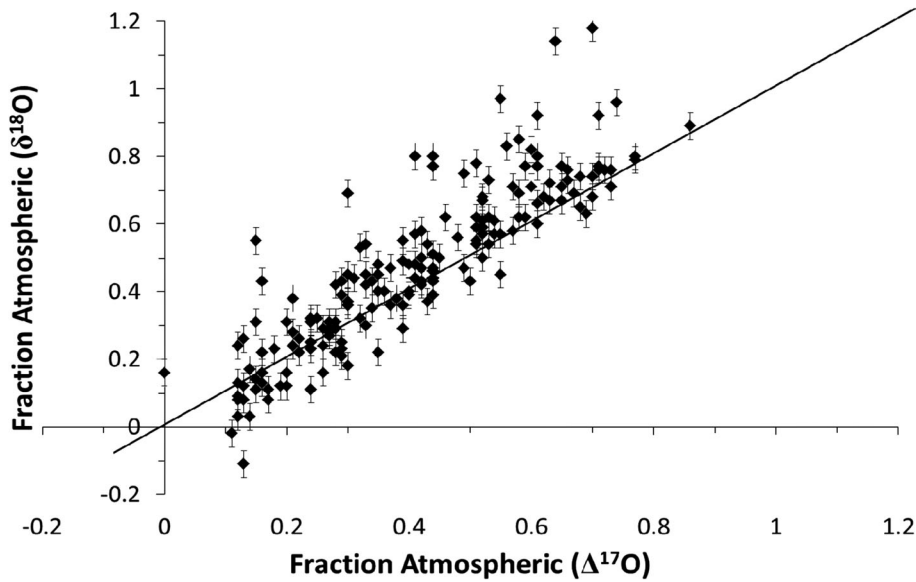


Figure 6. Mass balance estimates of the fraction atmospheric NO_3^- in runoff samples using an average $\text{NO}_3^-_{\text{atmo}}$ $\delta^{18}\text{O} = 57\text{‰}$ and $\Delta^{17}\text{O} = 24.3\text{‰}$ and a nitrification NO_3^- $\delta^{18}\text{O}$ of 3.5‰ and $\Delta^{17}\text{O} = -0.1\text{‰}$. Solid 1:1 correlation line represents if the $\delta^{18}\text{O}$ method and $\Delta^{17}\text{O}$ method gives the same fraction of atmospheric NO_3^- contribution. Error bars represent the possible range of nitrification $\delta^{18}\text{O}$ values based on local variation in water $\delta^{18}\text{O}$ values.

expected. The urbanized catchments had the lowest variance between estimation methods (MD— $r^2 = 0.82$, MX₁— $r^2 = 0.80$, CM— $r^2 = 0.72$, LD— $r^2 = 0.77$), whereas the two sites with the largest areas of open space (NU and MX₂) had the greatest variance between estimation methods (NU— $r^2 = 0.10$, MX₂— $r^2 = 0.52$) and had the largest underestimations of f_{atm} (NU—0.27, MX₂—0.15). This increase in variance with increasing soil surface area lends some support to the hypothesis that variability in the $\delta^{18}\text{O}_{\text{nit}}$ values is contributing to deviation in calculated f_{atm} when using runoff NO_3^- $\delta^{18}\text{O}$ values instead of the $\Delta^{17}\text{O}$ values. Additionally, this finding indicates that nitrification is more important in catchments with a large fraction of its surface area as exposed soil (relative to impervious surfaces) lending support to our expectations that nitrification rates in urban environments are a function of impervious surface area that decreases N turnover rate.

Biologically Processed NO_3^- Contribution

Although the presence of a significant f_{bio} NO_3^- across all catchments is not surprising, it is remarkable that this holds true for the CM catchment ($f_{\text{bio}} = 0.51 \pm 0.1$) which is 90.7% impervious (Figure 4). The large f_{bio} is likely due to nitrification occurring in soil particles deposited as dust between storms. The f_{bio} could be derived from

grass medians in the parking lots and a few small areas of exposed soil located within the watershed. However, these potential nitrification sources are scattered throughout the catchment and should appear as biogenic NO_3^- “pulses” in runoff, depending on their hydrologic connectivity to the remainder of the watershed (that is, runoff arrival time to the sampler). This result is not observed; rather, there is consistently greater than 30% biologic fraction throughout the runoff event suggesting that either (1) biologic sources of NO_3^- are evenly distributed across the catchment, or (2) f_{bio} NO_3^- increases in storm runoff because of in-stream nitrification.

Contribution of $[\text{NO}_3^-]_{\text{bio}}$ might source from nitrification occurring in dust particles previously deposited on impervious surfaces. It has been shown that ammonia oxidizing bacteria can attach and colonize soil aggregates (Prosser 2011), thus nitrification could proceed if there is NH_4^+ within the dust. NH_4^+ may have been concentrated on soil particulate matter after its entrainment in the atmosphere by reacting with atmospheric $\text{NH}_3(\text{g})$ and then nitrified after deposition. If true, the ratio of $\text{NH}_4^+/\text{NO}_3^-$ in wet deposition should be higher compared to the ratio in runoff (wet + dry deposition) due to loss of NH_4^+ during nitrification occurring since the last storm. For the CM catchment, the average ratio of $\text{NH}_4^+/\text{NO}_3^-$ in wet deposition was 0.96 whereas in runoff it was 0.75. The 0.21 difference nearly matches the 0.30

nitrification fraction (weighted by concentration) observed suggesting that nitrification is occurring between storm events. This is consistent with results from other studies in northern Arizona (Sullivan and others 2012) and the California Mediterranean grasslands (Parker and Schimel 2011), where equal or greater potential nitrification rates were measured in the dry season compared to the wet season. Volatilization of NH_4NO_3 from the surface would not decrease the ratio because HNO_3 is also lost during volatilization. Decreases in the $\text{NH}_4^+/\text{NO}_3^-$ ratio as a function of stream length in semi-arid, urban watersheds have been interpreted as in-stream nitrification (Welter and others 2005). If true at the CM site, we would expect to see an increase in the biologic fraction as a function of runoff arrival time. However, this was not observed in CM or in any of the study catchments, and is consistent with the finding by Gallo and others (2012), who showed that storm runoff residence times are not long enough for water column processes to significantly alter runoff hydrochemistry. We conclude then that the most robust explanation of a substantial f_{bio} is nitrification of intra-storm dry-deposited dust. Thus, although impervious surface area may limit water soil interactions and reduce N cycling, it does not completely eliminate it.

Isotope Assessment of Non-atmospheric NO_3^- Sources and NO_3^- Processing

To improve the understanding of nitrogen cycling dynamics in semi-arid urban streams, it is important to know the source of non-atmospheric NO_3^- . It has been suggested that the dual-isotope technique, where the NO_3^- $\delta^{15}\text{N}$ and $\delta^{18}\text{O}$ values are used in an isotope mixing plot (Kendall and others 2007) can help constrain the relative importance of N and/or NO_3^- sources. Transforming the $\delta^{15}\text{N}$ and $\delta^{18}\text{O}$ values using $\Delta^{17}\text{O}$ eliminates the atmospheric NO_3^- contribution in runoff and narrows the range of other possible NO_3^- sources. The transformed non-atmospheric NO_3^- $\delta^{15}\text{N}$ and $\delta^{18}\text{O}$ values were highly variable, and many fell outside the previous published ranges (-10 to 25%) (Figure 4; Table S2). However, the majority of non-atmospheric NO_3^- $\delta^{15}\text{N}$ values fell in a range that suggests it was comprised primarily of nitrified soil NH_4^+ and mineralized soil N. $\delta^{15}\text{N}$ values falling outside of this range could be the result of the depletion/enrichment in ^{15}N during NH_4^+ and NO_3^- volatilization in between rain events leading to higher $\delta^{15}\text{N}$ values in NO_3^- and lower $\delta^{15}\text{N}$ values in NH_3 , which are subsequently nitrified upon the next

rain event. $\delta^{18}\text{O}$ values were considerably higher than normal terrestrial sources.

Only a few samples had jointly elevated $\delta^{15}\text{N}$ and low $\delta^{18}\text{O}$ values characteristic of the nitrification of manure or sewage N. This is not surprising because in Tucson the storm water and sewer system infrastructure are separate entities and therefore septic or manure derived NO_3^- would not be expected to flow into in these catchments. Although there are some septic tanks and urban animal husbandry operations within the Tucson basin which might contribute to N loading in runoff, our data do not suggest widespread contribution. There were only a couple of data points that fell within the narrow range of synthetic NO_3^- fertilizers, which might reflect instances of higher N loading from fertilized trees and vegetation in residential and commercial parcels. Only one catchment (MX₁) had agricultural land use but neither this catchment nor any of the others showed a strong signal of fertilizer NO_3^- . This may be because Tucson urban landscapes are predominately xeric and leguminous, which do not typically require N additions.

The dual-isotope approach can also be used to differentiate between denitrification and assimilation NO_3^- losses (Boettcher and others 1990; Sebilo and others 2003). Understanding NO_3^- loss by denitrification is important because it removes nitrogen from the system, which reduces downstream contamination potential of recharged groundwater. If denitrification occurs then both the $\delta^{15}\text{N}$ and $\delta^{18}\text{O}$ of the residual NO_3^- would increase along a trend line with a mean slope of 0.5 (Chen and MacQuarrie 2005; Kendall 1998b), however, the $\epsilon\text{O}:\epsilon\text{N}$ has been observed between 0.47 and 0.77 (Groffman and others 2006). Conversely, assimilation by plants or microbes acts as a temporary holding reservoir for NO_3^- , which can then be regenerated by mineralization/nitrification downstream. If assimilation is taking place, both the $\delta^{15}\text{N}$ and $\delta^{18}\text{O}$ of the residual NO_3^- will increase along a trend line with a slope of 1 (Granger and others 2004). The relative importance of these two loss processes can be inferred using these two different isotope slopes, however, this is usually only feasible in confined spaces (for example, aquifers). Event-based dual-isotope plots were noisy and neither assimilation nor denitrification were detected in any of the watersheds.

Gross Nitrification

The GNR support the hypothesis that soil surface area (non-impervious areas) and N residence time

are the key factors controlling nitrification in these Tucson catchments. The highest GNR is in the NU catchment ($10.15 \pm 1 \text{ kg NO}_3\text{-N km}^{-2} \text{ day}^{-1}$) whereas CM had significantly lower GNR ($3.04 \pm 2 \text{ kg NO}_3\text{-N km}^{-2} \text{ day}^{-1}$) (Tables 2, S3). These findings would be expected based on our hypothesis: NU has highest soil surface and CM has the least. Although MX₂ has a soil surface area in-between these two extremes, it has a GNR similar to NU, which must be related to catchment characteristics, which enhances nitrification. The remaining three catchments (LD, MD, and MX₁) have similar GNR and soil surface areas. Only a few studies have reported gross nitrification rates of semi-arid systems because studies often focus on net nitrification rates. However, studies that have measured GNR were conducted on intact soil cores in the field, using ¹⁵N dilution has shown that GNR is dependent on water pulses, depth to wetting, and time since last wetting (Dijkstra and others 2012; Saetre and Stark 2005). In the semi-arid Central Plains Experimental Range (Colorado), gross nitrification rates were highest after 3 days following an initial wetting ($220\text{--}360 \text{ kg NO}_3^- \text{ km}^{-2} \text{ day}^{-1}$) and rates were near negligible after 10 days (Dijkstra and others 2012). Those GNR are similar to those observed GNR in forested ecosystems in New Mexico and Oregon which ranged from 25 to $300 \text{ kg NO}_3^- \text{ km}^{-2} \text{ day}^{-1}$ (Stark and Hart 1997). The GNR in forested and central plains are 5–100 times larger than those observed in Tucson's semi-arid, urbanized catchments.

The GNR reported here are similar to those reported in a Japanese mineral forest soil ($0\text{--}61 \text{ kg NO}_3^- \text{ km}^{-2} \text{ day}^{-1}$) (Kuroiwa and others 2011) and may be controlled by soil C:N ratios. It was

suggested that the low GNR in mineral forests was due to competition between immobilization and nitrification of NH_4^+ . They concluded that low soil C:N ratios controlled gross autotrophic nitrification by regulating gross NH_4^+ production rates (Kuroiwa and others 2011) and below a critical C:N ratio (15–20) gross autotrophic nitrification ceased (heterotrophic nitrification was determined to be negligible). Our urban catchments had C:N ratios ranging from 10 to 13 (*unpublished data*) suggesting slow gross NH_4^+ production rates that in turn lead to very low GNR. Also, another notable difference is that past GNR studies used soil core experiments, which require assumptions about ecosystem soil heterogeneity and its impact on GNG, whereas the current estimate of GNR is at the catchment scale and represents GNR across all landscapes. In addition, other controlled GNR experiments were conducted to determine the effect of pulsed water events or the competition between microbes and plants whereas here we have an integrated effect with multiple mediums within the catchment (for example, different soils textures, vegetation, and impervious surfaces) that may not have all received precipitation at the same intervals. We emphasize that non-natural N sources, such as sewage N or septic N, can also be nitrified and would be included in the GNR estimate. Given the already low GNR in these waters, this would suggest that sewage and septic are not significant sources of NO_3^- in the ephemeral stream. This may be due to their absence or poor hydrologic conductivity between surface water and ground water during transient events. Many of these effects have yet to be studied at the catchment scale and can all contribute to varying GNR.

Table 2. Mean (\pm SD) of Catchment-Based Gross Nitrification Rates Calculated Using Average Fractional Atmospheric Contribution

Catchment	Predominant land cover	Catchment area (km ²)	Impervious cover (%)	<i>n</i>	Dry deposition (kg N k ⁻¹ m ⁻² d ⁻¹)	Wet deposition (kg N k ⁻¹ m ⁻² d ⁻¹)	Total deposition (kg N k ⁻¹ m ⁻² d ⁻¹)	Gross nitrification rate (kg N k ⁻¹ m ⁻² d ⁻¹)
NU	Non-Urban	26.98	2.92	2	1.2	1.3 (\pm 0.3)	2.5 (\pm 0.3)	10.15 (\pm 1)
LD	Low Density	4.44	21.84	3	1.2	2.8 (\pm 2)	4.0 (\pm 2)	4.68 (\pm 2)
MD	Medium Density	0.45	40.64	5	1.2	2.0 (\pm 2)	3.2 (\pm 2)	6.21 (\pm 2)
MX ₁	Mixed Density	4.70	45.78	3	1.2	1.3 (\pm 1)	2.5 (\pm 1)	5.87 (\pm 4)
MX ₂	Mixed Density	25.30	50.63	4	1.2	1.8 (\pm 0.3)	3 (\pm 0.3)	6.22 (\pm 5)
CM	Commercial	0.33	90.70	5	1.2	1.9 (\pm 2)	3.1 (\pm 2)	3.04 (\pm 2)

n is the number of events per catchment. NO_3^- dry deposition rate was assumed to be constant (Fenn and others 2003b). NO_3^- wet deposition was obtained from event-based precipitation [NO_3^-] and normalized time between rain events.

In nearby urbanized Phoenix, urbanization and its subsequent land conversion from desert to lawns significantly increased soil N_2O emissions (by-product of both nitrification and denitrification) and N cycling (Hall and others 2008). Similarly, throughout the Tucson metropolitan area, some of the highest N_2O fluxes immediately following wetting of ephemeral streambeds ($3121 \mu\text{g N}_2\text{O-N m}^{-2} \text{h}^{-1}$) have been reported (Gallo and others 2013c). Semi-arid landscapes of low elevation (for example, riparian zones, ephemeral washes) provide “hot spots” and “hot moments” of potential denitrification due to patchiness in soil resources (for example, pooling of microbial biomass, nutrient resources, and water) (Harms and Grimm 2008). These studies’ conclusions combined with the observed low GNR suggest that less nitrified NO_3^- is present in urban catchments due to competing N cycling processes or that nitrification processes are “leaky” in which complete conversion of NH_3 to NO_3^- does not occur. Observed higher GNR in the Eastern U.S. are further evidence of the lack of atmospheric NO_3^- contributions in forested ecosystems where microbial turnover is higher therefore “erasing” atmospheric $\delta^{18}\text{O}$ contributions. In Tucson, gross nitrification rates are significantly lower and therefore atmospheric NO_3^- contributions prevail.

CONCLUSION

Here we show for the first time, the fractional contributions of atmospherically versus biologically derived NO_3^- in semi-arid urban environments. Urban runoff showed a significant fraction of atmospherically derived NO_3^- from all catchments (0–0.82, mean = 0.38) with higher fractions from more impervious catchments and lower from non-urban catchments. Our results are in agreement with the previous “build and flush” model for both NO_3^- fractions (Lewis and Grimm 2007). It was observed that during dry periods, atmospheric NO_3^- was depositing and accumulating on surfaces and as well as biologic NO_3^- (produced via nitrification) in soils and were subsequently flushed to waterways following the next rainfall/runoff event. The results presented here suggest increased impervious surface area allows for more atmospheric NO_3^- to reach urban waterways due to inefficient N cycling within the catchment. Whereas increased soil surfaces in catchments allow for nitrification and therefore atmospheric NO_3^- deposition is not as prevalent. The continued urban sprawl and further modification of ephemeral streams to augment a limited water

supply in semi-arid regions will continue to modify N cycling.

ACKNOWLEDGMENTS

This study was supported by National Science Foundation (NSF) DEB 0918708 and EF1063362. Dr. Kathleen Lohse was supported by the National Science Foundation under Award Number EPS-0814387.

REFERENCES

- Adams MB. 2003. Ecological issues related to N deposition to natural ecosystems: research needs. *Environ Intern* 29(2–3):189–99.
- Arnold CL, Gibbons CJ. 1996. Impervious surface coverage—the emergence of a key environmental indicator. *J Am Plan Assoc* 62(2):243–58.
- Austin AT, Yahdjian L, Stark JM, Belnap J, Porporato A, Norton U, Ravetta DA, Schaeffer SM. 2004. Water pulses and biogeochemical cycles in arid and semiarid ecosystems. *Oecologia* 141(2):221–35.
- Barnes RT, Raymond PA, Casciotti KL. 2008. Dual isotope analyses indicate efficient processing of atmospheric nitrate by forested watersheds in the northeastern U.S. *Biogeochemistry* 90(1):15–27.
- Berman T, Bronk DA. 2003. Dissolved organic nitrogen: a dynamic participant in aquatic ecosystems. *Aquat Microb Ecol* 31(3):279–305. doi:10.3354/ame031279.
- Boettcher J, Strebel O, Voerkelius S, Schmidt HL. 1990. Using isotope fractionation of nitrate-nitrogen and nitrate-oxygen for evaluation of microbial denitrification in a sandy aquifer. *J Hydrol* 114(3–4):413–24.
- Bunton CA, Llewellyn DR, Stedman G. 1959. 116. Oxygen exchange between nitrous acid and water. *J Chem Soc* 1959:568–73.
- Burns DA, Boyer EW, Elliott EM, Kendall C. 2009. Sources and transformations of nitrate from streams draining varying land uses: evidence from dual isotope analysis. *J Environ Qual* 38:1149–59.
- Campbell JL, Mitchell MJ, Mayor B. 2006. Isotopic assessment of NO_3^- and SO_4^{2-} mobility during winter in two adjacent watersheds in the Adirondack Mountains, New York. *J Geophys Res* 111:G04007.
- Carle MV, Halpin PN, Stow CA. 2005. Patterns of watershed urbanization and impacts on water quality. *J Am Water Resour Assoc* 41(3):693–708.
- Casciotti KL, Sigman DM, Hastings MG, Bohlke JK, Hilkert A. 2002. Measurement of the oxygen isotopic composition of nitrate in seawater and freshwater using the denitrifier method. *Anal Chem* 74(19):4905–12.
- Chang CCY, Kendall C, Silva SR, Battaglin WA, Campbell DH. 2002. Nitrate stable isotopes: tools for determining nitrate sources among different land uses in the Mississippi River Basin. *Can J Fish Aquat Sci* 59:1874–85.
- Chen DJZ, MacQuarrie KTB. 2005. Correlation of $\delta^{15}\text{N}$ and $\delta^{18}\text{O}$ in NO_3^- during denitrification in groundwater. *J Environ Eng Sci* 4(3):221–6. doi:10.1139/s05-002.
- Darrouzet-Nardi A, Erbland J, Bowman WD et al. 2012. Landscape-level nitrogen import and export in an ecosystem with

- complex terrain, Colorado Front Range. *Biogeochemistry* 109:271–85. doi:10.1007/s10533-011-9625-8.
- Davidson ES. 1973. *Geohydrology and water resources of the Tucson Basin, Arizona*, edited by United States Geological Survey. Washington, DC: United States Government Printing Office.
- Dejwakh NR, Meixner T, Michalski G, McIntosh J. 2012. Using ^{17}O to investigate nitrate sources and sinks in a semi-arid groundwater system. *Environ Sci Technol* 46:745–51.
- Diem JE, Comrie AC. 2001. Allocating anthropogenic pollutant emissions over space: application to ozone pollution management. *J Environ Manag* 63:425–47.
- Dijkstra FA, Augustine DJ, Brewer P, von Fischer JC. 2012. Nitrogen cycling and water pulses in semiarid grasslands: are microbial and plant processes temporally asynchronous? *Ecosyst Ecol* 170:799–808.
- Durka W, Schulze E-D, Gebauer G, Voerkelius S. 1994. Effects of forest decline on uptake and leaching of deposited nitrate determined from ^{15}N and ^{18}O measurements. *Nature* 372:765–7.
- Elliott EM, Kendall C, Boyer EW, Burns DA, Lear GG, Golden HE, Harlin K, Bytnerowicz A, Butler TJ, Glatz R. 2009. Dual nitrate isotopes in dry deposition: utility for partitioning NO_x source contributions to landscape nitrogen deposition. *J Geophys Res* 114:G04020.
- Ezcurra E. 2006. *Global deserts outlook*. Nairobi: United Nations Environment Programme.
- Fenn ME, Baron JS, Allen EB, Rueth HM, Nydick KR, Geiser L, Bowman WD, Sickman JO, Meixner T, Johnson DW, Neitlich P. 2003a. Ecological effects of nitrogen deposition in the western United States. *Bioscience* 53(4):404–20.
- Fenn ME, Haeuber R, Tonnesen GS, Baron JS, Grossman-Clarke S, Hope D, Jaffe DA, Copeland S, Geiser L, Rueth HM, Sickman JO. 2003b. Nitrogen emissions, deposition, and monitoring in the Western United States. *Bioscience* 53(4):391–403.
- Freyer HD. 1991. Seasonal-variation of $^{15}\text{N}/^{14}\text{N}$ ratios in atmospheric nitrate species. *Tellus B* 43(1):30–44.
- Gallo EL, Lohse KA, Brooks PD, McIntosh JC, Meixner T, McLain JET. 2012. Quantifying the effects of stream channels on storm water quality in a semi-arid urban environment. *J Hydrol* 470–471:98–110.
- Gallo EL, Brooks PD, Lohse KA, McLain JET. 2013a. Land cover controls on summer discharge and runoff solution chemistry of semi-arid urban catchments. *J Hydrol* 485:37–53. doi:10.1016/j.jhydrol.2012.11.054.
- Gallo EL, Brooks PD, Lohse KA, McLain JET. 2013b. Temporal patterns and controls on runoff magnitude and solution chemistry of urban catchments in the semiarid southwestern United States. *Hydrol Process* 27(7):995–1010. doi:10.1002/hyp.9199.
- Gallo EL, Lohse KA, Brooks PD, Ferlin CM, Meixner T. 2013c. Physical and biological controls on biogeochemical processes of semi-arid urban ephemeral waterways. *Biogeochemistry*. doi:10.1007/s10533-013-9927-0.
- Garcia M, Peters-Lidard CD, Goodrich DC. 2008. Spatial interpolation of precipitation in a dense gauge network for monsoon storm events in the southwestern United States. *Water Resour Res* 44(5):W05S13.
- Gaziz C, Feng X. 2004. A stable isotope study of soil water: evidence for mixing and preferential flow paths. *Geoderma* 119:97–111.
- Gelt J, Henderson J, Seasholes K, Tellman B, Woodard G, Carpenter K, Hudson C, Sherif S. 1999. *Water in the Tucson area: seeking sustainability*. Tucson: The University of Arizona, Water Resources Research Center. pp 1–55.
- Goodale CL, Thomas SA, Fredriksen G, Elliott EM, Flinn KM, Butler TJ, Walter MT. 2009. Unusual seasonal patterns and inferred processes of nitrogen retention in forested headwaters of the Upper Susquehanna River. *Biogeochemistry* 93:197–218.
- Granger J, Sigman DM. 2009. Removal of nitrite with sulfamic acid for nitrate N and O isotope analysis with the denitrifier method. *Rapid Commun Mass Spectr* 23:3753–62.
- Granger J, Sigman DM, Needoba JA, Harrison PJ. 2004. Coupled nitrogen and oxygen isotope fractionation of nitrate during assimilation by cultures of marine phytoplankton. *Limnol Oceanogr* 49(5):1763–73.
- Groffman PM, Law NL, Belt KT, Band LE, Fisher GT. 2004. Nitrogen fluxes and retention in urban watershed ecosystems. *Ecosystems* 7(4):393–403.
- Groffman PM, Altabet MA, Böhlke JK, Butterbach-Bahl K, David MB, Firestone MK, Giblin AE, Kana TM, Nielsen LP, Voytek MA. 2006. Methods for measuring denitrification: diverse approaches to a difficult problem. *Ecol Appl* 16(6):2091–122.
- Hall SJ, Huber D, Grimm NB. 2008. Soil N_2O and NO emissions from an arid, urban ecosystem. *J Geophys Res* 113:G01016.
- Hall SJ, Sponseller R, Grimm NB, Huber D, Kaye JP, Clark C, Collins SL. 2011. Ecosystem response to nutrient enrichment across an urban airshed in the Sonoran Desert. *Ecol Appl* 21(3):640–60.
- Harms TK, Grimm NB. 2008. Hot spots and hot moments of carbon and nitrogen dynamics in a semiarid riparian zone. *J Geophys Res* 113:G01020.
- Hatt BE, Fletcher TD, Walsh CJ, Taylor SL. 2004. The influence of urban density and drainage infrastructure on the concentrations and loads of pollutants in small catchments. *Environ Manag* 34(1):112–24.
- Horibe Y, Shigehara K, Takakuwa Y. 1973. Isotopic separation factors of carbon-dioxide–water system and isotopic composition of atmospheric oxygen. *J Geophys Res* 78:2625–9.
- Kaiser J, Hastings MG, Houlton BZ, Rockmann T, Sigman DM. 2007. Triple oxygen isotope analysis of nitrate using the denitrifier method and thermal decomposition of N_2O . *Anal Chem* 79(2):599–607.
- Kaushal SS, Groffman PM, Band LE, Elliott EM, Shields CA, Kendall C. 2011. Tracking nonpoint source nitrogen pollution in human-impacted watersheds. *Environ Sci Technol* 45:8225–32.
- Kendall C. 1998a. Tracing nitrogen sources and cycling in catchments. In: Kendall C, McDonnell JJ, Eds. *Isotope tracers in catchment hydrology*. Amsterdam: Elsevier. p 519–76.
- Kendall C. 1998b. Tracing nitrogen sources and cycling in catchments. In: Kendall C, McDonnell JJ, Eds. *Isotope tracers in catchment hydrology*. Amsterdam: Elsevier Science. p 519–76.
- Kendall C, Elliott EM, Wankel SD. 2007. Tracing anthropogenic inputs of nitrogen to ecosystems. In: Michener RH, Lajtha K, Eds. *Stable isotopes in ecology and environmental science*. Malden: Blackwell. p 375–449.
- Kroopnick P, Craig H. 1972. Atmospheric oxygen: isotopic composition and solubility fractionation. *Science* 175:54–5.
- Kuroiwa M, Koba K, Isobe K, Tateno R, Nakanishi A, Inagaki Y, Toda H, Otsuka S, Senoo K, Suwa Y, Yoh M, Urakawa R, Shibata H. 2011. Gross nitrification rates in four Japanese forest soils: heterotrophic versus autotrophic and the regulation factors for the nitrification. *J For Res* 16:363–73.

- Lewis DB, Grimm NB. 2007. Hierarchical regulation of nitrogen export from urban catchments: interactions of storms and landscapes. *Ecol Appl* 17(8):2347–64.
- Lohse KA, Hope D, Sponseller R, Allen JO, Grimm NB. 2008. Atmospheric deposition of carbon and nutrients across an arid metropolitan area. *Sci Total Environ* 402:95–105.
- Lovett GM, Jones CG, Turner MG, Weathers KC. 2005. Ecosystem function in heterogeneous landscapes. New York: Springer.
- Mayer B, Bollwerk SM, Mansfeldt T, Hutter B, Veizer J. 2001. The oxygen isotope composition of nitrate generated by nitrification in acid forest floors. *Geochim Cosmochim Acta* 65(16):2743–56.
- Mayer B, Boyer EW, Goodale CL, Jaworski NA, Van Breemen N, Howarth RW, Seitzinger S, Billen G, Lajtha K, Nadelhoffer K, Van Dam D, Hetling LJ, Nosal M, Paustian K. 2002. Sources of nitrate in rivers draining sixteen watersheds in the northeastern U.S.: isotopic constraints. *Biogeochemistry* 57(58):171–97.
- McCrackin ML, Harms TK, Grimm NB, Hall SJ, Kaye JP. 2008. Responses of soil microorganisms to resource availability in urban, desert soils. *Biogeochemistry* 87(2):143–55.
- Michalski G, Scott Z, Kabiling M, Thiemens M. 2003a. First measurements and modelling of $\Delta^{17}\text{O}$ in atmospheric nitrate. *Geophys Res Lett* 30(16):1870.
- Michalski G, Scott Z, Kabiling M, Thiemens M. 2003b. First measurements and modeling of $\Delta^{17}\text{O}$ in atmospheric nitrate. *Geophys Res Lett* 30(16):1870.
- Michalski G, Meixner T, Fenn M, Hernandez L, Sirulnik A, Allen E, Thiemens M. 2004a. Tracing atmospheric nitrate deposition in a complex semiarid ecosystem using $\Delta^{17}\text{O}$. *Environ Sci Technol* 38(7):2175–81.
- Michalski G, Meixner T, Fenn M, Hernandez L, Sirulnik A, Allen E, Thiemens M. 2004b. Tracing atmospheric nitrate deposition in a complex semiarid ecosystem using $\Delta^{17}\text{O}$. *Environ Sci Technol* 38(7):2175–81.
- Miller MF. 2002. Isotopic fractionation and the quantification of ^{17}O anomalies in the oxygen three-isotope system: an appraisal and geochemical significance. *Geochim Cosmochim Acta* 66(11):1881–9.
- Morin E, Goodrich DC, Maddox RA, Gao X, Gupta HV, Sorooshian S. 2006. Spatial patterns in thunderstorm rainfall events and their coupling with watershed hydrological response. *Adv Water Resour* 29(6):843–60.
- Morin S, Savarino J, Frey MM, Domine F, Jacobi HW, Kaleschke L, Martins JMF. 2009. Comprehensive isotopic composition of atmospheric nitrate in the Atlantic Ocean boundary layer from 65 degrees S to 79 degrees N. *J Geophys Res* 114:D05303. doi:10.1029/2008JD010696.
- Munger JW, Fan SM, Bakwin PS, Goulden ML, Goldstein AH, Colman AS, Wofsy SC. 1998. Regional budgets for nitrogen oxides from continental sources: Variations of rates for oxidation and deposition with season and distance from source regions. *J Geophys Res* 103(D7):8355–68.
- Norman LM, Feller M, Guertin DP. 2009. Forecasting urban growth across the United States–Mexico border. *Comput Environ Urban Syst* 33(2):150–9.
- Pardo LH, Kendall C, Pett-Ridge J, Chang CCY. 2004. Evaluating the source of streamwater nitrate using $\delta^{15}\text{N}$ and $\delta^{18}\text{O}$ in nitrate in two watersheds in New Hampshire, USA. *Hydrol Process* 18:2699–712.
- Parker SS, Schimel JP. 2011. Soil nitrogen availability and transformations differ between the summer and the growing season in a California grassland. *Appl Soil Ecol* 48:185–92.
- Prosser JI. 2011. Soil nitrifiers and nitrification. In: Ward BB, Arp DJ, Klotz MG, Eds. *Nitrification*. New York: American Society for Microbiology. p 347–62.
- Riha, K. 2013. The use of stable isotopes to constrain the nitrogen cycle. PhD Dissertation, Purdue University.
- Saetre P, Stark JM. 2005. Microbial dynamics and carbon and nitrogen cycling following re-wetting of soils beneath two semi-arid plant species. *Oecologia* 142(2):247–60.
- Sebestyen SD, Boyer EW, Shanley JB, Kendall C, Doctor DH, Aiken GR, Ohte N. 2008. Sources, transformations, and hydrological processes that control stream nitrate and dissolved organic matter concentrations during snowmelt in an upland forest. *Water Resour Res* 44:12.
- Sebilio M, Billen G, Grably M, Mariotti A. 2003. Isotopic composition of nitrate-nitrogen as a marker of riparian and benthic denitrification at the scale of the whole Seine River system. *Biogeochemistry* 63:35–51.
- Snider DM, Spoelstra J, Schiff SL, Venkiteswaran JJ. 2010. Stable oxygen isotope ratios of nitrate produced from nitrification: ^{18}O -labeled water incubations of agricultural and temperate forest soils. *Environ Sci Technol* 44:5358–64.
- Spoelstra J, Schiff SL, Elgood RJ, Semkin RG, Jeffries DS. 2001. Tracing the sources of exported nitrate in the Turkey Lakes watershed using $^{15}\text{N}/^{14}\text{N}$ and $^{18}\text{O}/^{16}\text{O}$ isotopic ratios. *Ecosystems* 4:536–44.
- Stark JM, Hart SC. 1997. High rates of nitrification and nitrate turnover in undisturbed coniferous forests. *Nature* 385(6611):61–4.
- Sullivan BW, Selmants PC, Hart SC. 2012. New evidence that high potential nitrification rates occur in soils during dry seasons: are microbial communities metabolically active during dry seasons? *Soil Biol Biogeochem* 53:28–31.
- Syed KH, Goodrich DC, Myers DE, Sorooshian S. 2003. Spatial characteristics of thunderstorm rainfall fields and their relation to runoff. *J Hydrol* 271(1–4):1–21.
- U.S. Census Bureau, Tucson, Arizona, 2012.
- U.S. Environmental Protection Agency, The National Emissions Inventory, 2012.
- Vitousek PM, Aber JD, Howarth RW, Likens GE, Matson PA, Schindler DW, Schlesinger WH, Tilman D. 1997. Human alteration of the global nitrogen cycle: sources and consequences. *Ecol Appl* 7:737–50.
- Walker GR, Hughes MW, Allison GB, Barnes CJ. 1988. The movement of isotopes of water during evaporation from a bare soil surface. *J Hydrol* 97:181–97.
- Welter JR, Fisher SG, Grimm NB. 2005. Nitrogen transport and retention in an arid land watershed: influence of storm characteristics on terrestrial–aquatic linkages. *Biogeochemistry* 76:421–40.
- Williard KWJ, DeWalle DR, Edwards PJ, Sharpe WE. 2001. ^{18}O isotopic separation of stream nitrate sources in mid-Appalachian forested watersheds. *J Hydrol* 252:174–88.
- Worsfold PJ, Monbet P, Tappin AD, Fitzsimons MF, Stiles DA, McKelvie ID. 2008. Characterisation and quantification of organic phosphorus and organic nitrogen components in aquatic systems: a review. *Anal Chim Acta* 624(1):37–58. doi:10.1016/j.aca.2008.06.016.
- Wright, WE. 2001. δD and $\delta^{18}\text{O}$ in mixed conifer systems in the U.S. Southwest: the potential of $\Delta^{18}\text{O}$ in *Pinus ponderosa* tree rings as a natural environmental recorder, PhD The University of Arizona, Ann Arbor, MI.